Chapter 4

Energy Management System for Smart Buildings under FDI Attack - Decentralized Approach

4.1 Introduction

The previous chapter discusses single smart home energy management system to minimize the energy cost considering battery degradation cost. In this chapter, a game-theory based multi-smart building energy management system has been proposed to minimize the energy cost considering False Data Injection (FDI) attack on the price data.

Due to the significant increase in energy demand in smart residential buildings, building energy management systems (BEMS) requires a coordination among energy management system of smart buildings and various controllable loads to reduce energy costs in smart building infrastructure. Also, scheduling of appliances in smart buildings plays a significant role in the minimization of energy cost in smart building energy management systems (SBEMS). Renewable Energy Sources (RESs) are installed in smart buildings to reduce the dependency on conventional energy resources. Combined heat and power (CHP) generators and Battery Storage Systems (BSSs) are also used to reduce the effects of intermittency of the RESs in the smart buildings. The utility provides a real time prices to guide the energy consumption in the prosumers system. Demand response (DR) programs are also used by the utility to shift the energy demand from peak hour to off-peak hour to reduce the electricity bill. Since the proposed SBEMS is linked to cyber-

physical system and Information Technology (IT) for communication purpose, there is a need for advanced and intelligent metering infrastructure for its secure operation.

Since the communication infrastructure includes IT as well as advance metering for controlling and scheduling of smart home appliances, it can be prone to cyber-attack. Therefore, cyber-attack is an important issue in the integrated residential building management system in the current smart grid infrastructure.

The coordinated smart building energy management considering demand scheduling program with cyber-attack is considered in few literature however, comprehensive analysis is not attempted. In this context, the effects of FDI attack on energy scheduling are rigorously analyzed in this work by exploring game-theory based smart building energy management system. Since FDI-attack detection is a post-facto analysis, resilience to FDI attack in load scheduling is essential to prevent impact of FDI attack while scheduling.

Proposed coordinated multi smart building energy management system incorporating resilient strategy against FDI-attack is a new contribution in this chapter. Further, the optimal scheduling of smart home appliances, taking into account the potential for power import and export between the grid and smart buildings, is proposed to reduce electricity bill. In the proposed work, minimization of electricity bill of each smart building is done incorporating resilience to the FDI-attack in the scheduling process. The main contributions of this chapter are listed as follows.

- An iterative method has been used for a game-theory based smart building energy management system to reduce individual electricity bills of smart building.
- A resilient scheduling strategy based on import and export power of grid is proposed for smart buildings to eliminate the impact of FDI attack in loads scheduling.
- The FDI attack is detected by looking at the difference in bills, i.e., the difference between estimated and actual bills, and the maximum change in demand, i.e., forecasted power and attacked power.

4.2 System Architecture

This study considers the game-theory based energy management of grid connected smart buildings. The architecture of the proposed system is depicted in Figure 4.1. The proposed

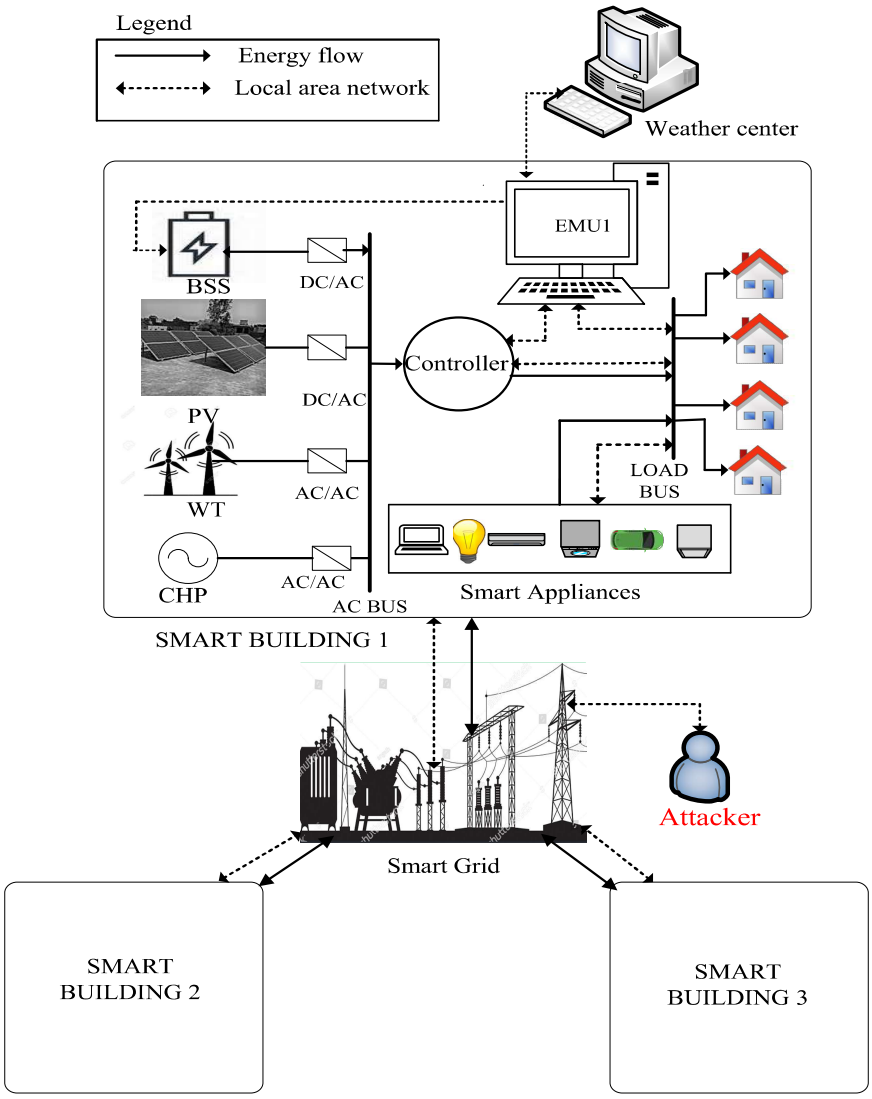

Figure 4.1: Architecture of SBEMS

system consists of three smart buildings, and each smart building has four smart homes with multiple smart appliances for energy consumption. Each smart building has different energy resources such as rooftop solar PV, wind turbines, battery storage systems (BSSs), and combined heat and power (CHP) generators. To reduce electricity bills and reliance on utility electricity, smart home consumers use solar PV, wind turbines and battery storage systems. To reduce the effect of variability in generation from RESs, battery storage systems are used to make game-theory based SBEMS more reliable.

Each smart home has different types of smart loads such as laptop, tumble dryer, vacuum cleaner, cooking hob, dish washer (DW) microwave, cooking oven, lighting bulb,

desktop, electric vehicle (EV), washing machine (WM) and refrigerator. Each smart building is equipped with a computer aided device, i.e. Local Energy Management Unit (EMU). It is used by respective operators to manage smart home appliances and generation resources in a smart building. Each smart building also has a smart controller which is connected to the smart grid, DER and smart devices. The Local Area Network (LAN) is used to communicate the price signal and power exchange requests between the Smart Buildings (SBs) and the utility.

4.3 Problem Formulation

4.3.1 Objective Function

In this work, each Smart Building (SB) aims to minimise its energy cost (electricity bill) in a game-theoretic environment under FDI attacks. The power exchange price for SBs depends on the base price set by the utility and power exchange strategies of all participating SBs. The EMU in each SB schedules the appliances of all smart homes, BSS and CHP generators under its purview based on the availability of RESs generation, power exchange strategies of other SBs and the base price set by the utility. Effect of FDI attacks on scheduling, detection of FDI attacks, and defence strategy against FDI attack have also been investigated in this work.

The energy cost minimisation objective for each of the SBs can be written as

$$Obj = min \sum_{t} C_b(t). \tag{4.1}$$

Here, $C_b(t)$ is the energy cost of b^{th} SB. The $C_b(t)$ consists of operating cost of BSS and CHP generator, and cost of power exchange with utility. The $C_b(t)$ can be defined as

$$C_b(t) = [P_b^{dis}(t) \times \lambda_{bmc} + P_b^{chp}(t) \times \lambda_g + C_b^{gex}(t)]. \tag{4.2}$$

Here, $P_b^{dis}(t)$ and $P_b^{chp}(t)$ are the discharged power from BSS and generated power from CHP generator during t^{th} interval for b^{th} SB. λ_{bmc} and λ_g are the battery maintenance price and natural gas price, respectively. For b^{th} SB, the cost of power exchange with utility, $C_b^{gex}(t)$, depends on the power exchange of b^{th} SB with utility, $P_b^{gex}(t)$, base price set by utility, $\lambda(t)$, and effective power exchange of other SBs except b^{th} smart building,

$P^{gex}_{-b}(t)$. The $C^{gex}_{b}(t)$ can be defined as

$$C^{gex}_{b}(t) = P^{gex}_{b}(t) \times \Bigg(\lambda(t) + 0.05 \times (P^{gex}_{b}(t) + P^{gex}_{-b}(t)) \Bigg). \tag{4.3}$$

FDI attack in utility price affects the cost of power exchange with utility. After FDI-attack, the power exchange cost of b^{th} SB can be written as

$$C^{gex}_{b}(t) = P^{gex}_{b}(t) \times \Bigg(\gamma(t) + 0.05 \times (P^{gex}_{b}(t) + P^{gex}_{-b}(t)) \Bigg), \tag{4.4}$$

where, $\gamma(t)$ is the attacked utility price.

Similarly, FDI-attack in power exchange signal also affects the cost of power exchange with utility. Attacker may alter the $P^{gex}_{-b}(t)$ as follows.

$$P^{gex}_{-ba}(t) = P^{gex}_{-b}(t) - G(\mu, \sigma), \tag{4.5}$$

where, $G(\mu, \sigma)$ is Gaussian noise. The power consumption of SH appliances depends on their operating status and their rated power as discussed in Chapter 2. The total power demand of h^{th} smart home during t^{th} interval, $P_h(t)$, is equal to the sum of power consumption of all the appliances (UNLs, SLs and TDLs) of that SH. The $P_h(t)$ can be defined as

$$P_h(t) = \sum_{a_i \in (a_u, a_s, a_{td})} P_{a_i}(t). \tag{4.6}$$

Where, a_u, a_s and a_{td} are the indices of UNLs, SLs and TDLs respectively. $P_{a_i}(t)$ is the power consumption of a^{th}_i appliance and it can be defined as

$$P_{a_i}(t) = \sum_{t} S_{a_i}(t) \times P_{rated,a_i}. \tag{4.7}$$

Where, S_{a_i} and P_{rated,a_i} are respectively the binary variable and rated power of a^{th}_i appliance. Similarly, the total heat demand of the h^{th} SH during t^{th} interval, $H_h(t)$, is equal to the sum of the heat required by all the appliances in that SH, can be written as,

$$H_h(t) = \sum_{i} H_i(t). \tag{4.8}$$

Here, $H_i(t)$ is the heat required by i^{th} appliance.

The total power demand of b^{th} smart building, $P_b(t)$, is equals to the sum of demand of all SHs in a smart building. The $P_b(t)$ can be written as,

$$P_b(t) = \sum_{h \in b} P_h(t). \tag{4.9}$$

The constraint on maximum limit of $P_b(t)$ by MDL, P_{mdl} can be expressed as,

$$P_b(t) \leq P_{mdl}. \tag{4.10}$$

The total power demand of b^{th} SB, $P_b(t)$, must be equal to algebraic sum of all the generations, power exchange with utility, charging power and discharging power of BSS which can be expressed as a load balancing constraint for b^{th} SB as follows.

$$P_b(t) = P_b^{chp}(t) + P_b^r(t) + P_b^{dis}(t) - P_b^{ch}(t) + P_b^{gex}(t) \tag{4.11}$$

Here, $P_b^{chp}(t)$ and $P_b^r(t)$ respectively are the power outputs of CHP generator and RESs in the b^{th} smart building. $P_b^{ch}(t)$ and $P_b^{dis}(t)$ are the battery charging and discharging power of BSS. The power exchange of b^{th} SB with the utility, $P_b^{gex}(t)$, can be written in terms of power import, $P_b^{imp}(t)$, and power export, $P_b^{exp}(t)$, as follows.

$$P_b^{gex}(t) = P_b^{gimp}(t) - P_b^{gexp}(t). \tag{4.12}$$

$P_b^{gimp}(t)$ and $P_b^{gexp}(t)$ can be bound through following constraints.

$$P_b^{gimp}(t) \leq P_b^{gimp,max} \times \alpha_b(t), \tag{4.13}$$

$$P_b^{gexp}(t) \leq P_b^{gexp,max} \times (1 - \alpha_b(t)), \tag{4.14}$$

where, $\alpha_b(t)$ is a binary variable which indicate the import/export status of b^{th} building (1 for power import and 0 for power export).

Eq. 4.15, describes that the output power of a CHP generator cannot exceed its rated capacity.

$$P_b^{chp}(t) \leq P_c^{chp} \tag{4.15}$$

Heat output of the CHP generator, $H_b^{chp}(t)$, depends on P_b^{chp} and specific parameters, P_{TE} (electrical power to heat ratio of CHP generator), as expressed bellow.

$$H_b^{chp}(t) = \frac{P_b^{chp}(t)}{P_{TE}}. \tag{4.16}$$

The operating temperature of a_{td}^{th} TDL, $T_{a_{td}}(t)$ should be within the pre-set range as follows,

$$T_{a_{td}}^{min} \leq T_{a_{td}}(t) \leq T_{a_{td}}^{max}, \tag{4.17}$$

where, $T_{a_{td}}^{min}$ and $T_{a_{td}}^{max}$ are the minimum and maximum temperature limit for a TDL, respectively.

BSS operations are subject to some constraints related to battery specifications and scheduling expressed through following equations.

$$SOC_b(t+1) = (1-\sigma) \times SOC_b(t) + P_b^{ch}(t) \times \eta^{ch} - P_b^{dis}(t)/\eta^{dis}, \tag{4.18}$$

$$SOC^{min} \leq SOC_b(t) \leq SOC^{max}, \tag{4.19}$$

$$P_b^{ch}(t) \leq P_{max,b}^{ch}(t) \times \alpha_{1,b}(t), \tag{4.20}$$

and

$$P_b^{dis}(t) \leq P_{max,b}^{dis}(t) \times (1 - \alpha_{1,b}(t)). \tag{4.21}$$

Here, $\alpha_{1,b}(t)$ is a binary variable for BSS of b^{th} SB; it has a value of 1 for charging and 0 for discharging. Eq. 4.18 describes the State-of-Charge (SOC) level of BSS at $(t+1)$ which depends on the SOC level, charging power, and discharging power at t. SOC limits of BSS are constrained by Eq. 4.19. The Eqs. 4.20 and 4.21 limit the charge and discharge power of the BSS according to the maximum rate of charge and discharge, respectively. These two constraints also ensure that simultaneous charging and discharging are restricted.

Similar to BSS, constraints related to thermal storage systems (TSS) can also be defined. For b^{th} SB, state-of-charge of TSS at $(t+1)$ can be calculated as,

$$SOC_b^T(t+1) = SOC_b^T(t) + P_b^{chT}(t) \times \eta^{chT} - P_b^{disT}(t)/\eta^{disT}, \tag{4.22}$$

where, $SOC_b^T(t)$, $P_b^{chT}(t)$, and $P_b^{disT}(t)$ are the SOC, charging, and discharging power of TSS at time t. The minimum and maximum limits on SOC^T are expressed as constraint in the following manner.

$$SOC^{T,min} \leq SOC_b^T(t) \leq SOC^{T,max}. \tag{4.23}$$

The restriction on simultaneous charging and discharging of TSS along with the bounds on charging and discharging power of TSS are expressed in Eqs. 4.24 and 4.25.

$$P_b^{chT}(t) \leq P_{max,b}^{chT} \times \alpha_{2,b}(t), \tag{4.24}$$

$$P_b^{disT}(t) \leq P_{max,b}^{disT} \times (1 - \alpha_{2,b}(t)). \tag{4.25}$$

Here, $\alpha_{2,b}$ is a binary variable ($\epsilon\{0,1\}$) for TSS of b^{th} smart building; it has a value of 1 for charging and 0 for discharging. $P_{max,b}^{chT}$ and $P_{max,b}^{disT}$ are the maximum charging and discharging power of TSS respectively of b^{th} smart building.

The thermal demand, $H_b^d(t)$, of b^{th} smart building must be balanced with the heat output of CHP, $H_b^{chp}(t)$, TSS charging heat, $H_b^{chT}(t)$, and TSS discharging heat, $H_b^{disT}(t)$, of b^{th} SB is as follows.

$$H_b^d(t) = H_b^{chp}(t) + H_b^{disT}(t) - H_b^{chT}(t), \tag{4.26}$$

where,

$$H_b^{disT}(t) = P_b^{disT}/\eta^{disT},$$
$$H_b^{chT}(t) = P_b^{chT}/\eta^{chT}.$$

4.3.2 Game-theory model

In this work, smart buildings (SBs) decide their strategy of power exchange with utility based on the electricity price set by utility. SBs also influence strategies of each other as discussed in section 4.3.1. In this non-cooperative game-theoretic model, each SB aims to minimize its energy cost while considering the strategies of the other SBs. The non-cooperative game can be defined as follows.

- Players: Number of SBs Q, $b \in Q$.
- Strategies: Power exchange with utility $P_b^{gex}(t)$, $\forall\ b \in Q$.
- Payoff: $U(P_b^{gex}, \boldsymbol{P_{-b}^{gex}}) \equiv U_b(t) = -C_b(t)$, $\forall\ b \in Q$,

where,

$$\boldsymbol{P_{-b}^{gex}} = [P_1^{gex}(t), P_2^{gex}(t), ..., P_{b-1}^{gex}(t), P_{b+1}^{gex}(t)...., P_Q^{gex}(t)]$$

is the strategy set at time t of all SBs except b^{th} SB. The Nash equilibrium of the game can be defined as,

$$U(P_b^{gex*}, \boldsymbol{P_{-b}^{gex*}}) \geq U(P_b^{gex}, \boldsymbol{P_{-b}^{gex*}}), \forall b \in Q. \tag{4.27}$$

4.3.3 Price and Bill Prediction

We have taken the time series price data of last three months to forecast the price data given in Table 4.1. Here, we have used Gaussian Process Regression (GPR) model to predict the price data [147]. Total 8640 samples of past time-series data are used for GPR modeling, out of which 60% and 40% of the total data set are used for training and testing

Table 4.1: Forecatsed Price

Time (Hour)	1	2	3	4	5	6	7	8	9	10	11	12	13	14	15	16	17	18	19	20	21	22	23	24
Forecasted Price(₹)	2.9	2.7	3	3	1.8	3	3.75	3.5	3.2	3	3.1	3.15	2.8	2.7	2.65	2.75	3	4.25	3.5	3.15	2.9	2.9	2.6	2.6
Recived Price(₹)	2.9	2.7	3	3	3.5	3	2.5	2.75	3.2	3	3.1	3.15	2.8	3	3.5	4	3.25	3	2.75	3	2.9	2.9	2.6	2.6

the GPR model, respectively, and 10% of the training data is used for model validation. L2 regularization and optimal hyper-parameters are used respectively to reduce model over-fitting and root mean square error (RMSE). The details of the price prediction using the GPR model are shown in Figure 4.2. The bill derived from the scheduling of smart appliances of SBs considering the predicted price is known as the reference bill, B^R.

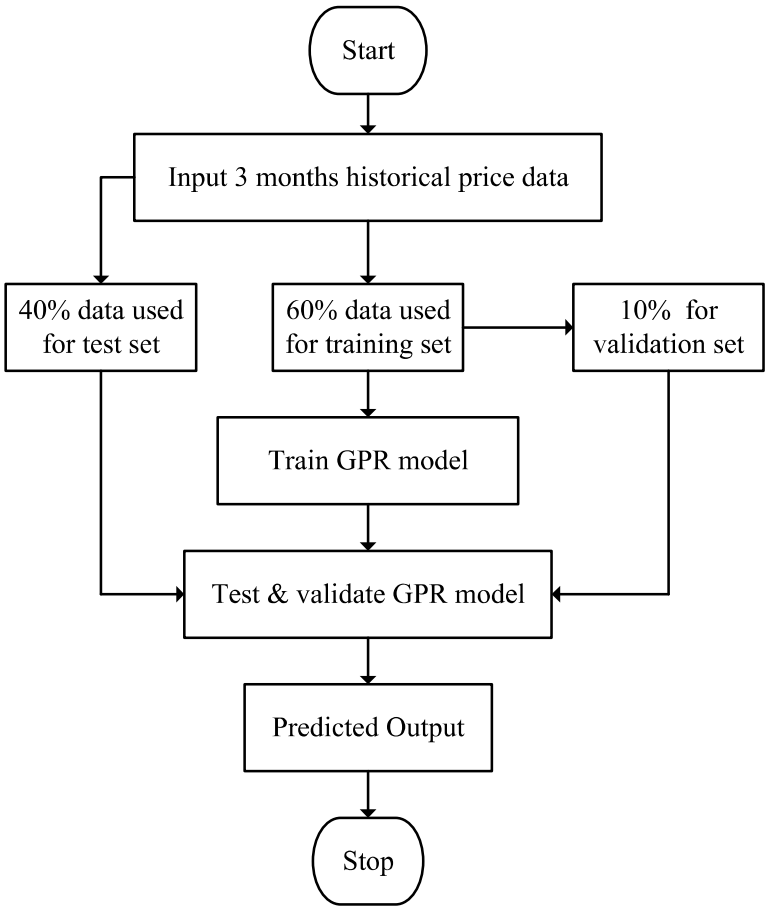

Figure 4.2: Flowchart showing Prediction of Electricity Price

4.3.4 Strategy of FDI Attack

In multiple smart buildings, there is a risk that any consumer (any smart building) will be able to attack the actual price of the utility for their own benefit. The actual price can be changed by the attacker by injecting some false data into the utility price. However, the user may be unable to find the actual change in utility price after the injection of false data. But users can reduce the impact of FDI attack on their scheduling to a certain level. Generally, consumers follow a similar daily load consumption pattern. Furthermore, the price of electricity may vary, but the shape of the price curve follows a similar pattern to the past few days. Both these assumptions can be used to detect FDI attacks. In our proposed work, GPR based forecasted price, considering price data of last three months, is used to predict the electricity consumption pattern $P_b^R(t)$ and the electricity bill B^R. Based on actual bill, B, and power demand, $P_b(t)$, a rate of change of electricity bill ΔB and rate of change in demand (maximum change in demand) can be calculated as,

$$\Delta B = \frac{B - B^R}{B^R}. \tag{4.28}$$

$$\Delta P(t) = P_b(t) - P_b^R(t). \tag{4.29}$$

If rate of change of electricity bill and maximum change in demand exceed tolerance limits, i.e., $|\Delta B| > \delta b$, or $|\Delta P| > \delta p$, then it indicates the possibility of FDI-attack in the price. In this case, following resilient scheduling constraints can be adopted to reduce the impact of FDI-attacks on scheduling.

$$0.9P_b^{gimp,R}(t) \leq P_b^{gimp}(t) \leq 1.1P_b^{gimp,R}(t). \tag{4.30}$$

$$0.9P_b^{gexp,R}(t) \leq P_b^{gexp}(t) \leq 1.1P_b^{gexp,R}(t). \tag{4.31}$$

Here, $P_b^{imp,R}(t)$ and $P_b^{exp,R}(t)$ are the reference values of grid import and export power, respectively, in t^{th} interval. Eq. (4.30) and Eq. (4.31) restrict the deviation of import and export power from reference value. Figure 4.3 describes the steps for detecting FDI attacks, and performing the resilient scheduling.

4.4 Results and Discussion

The proposed system has been validated by considering different smart home loads, RESs, CHP generators and BSSs. Different types of SH loads, viz. refrigerator, vacuum cleaner,

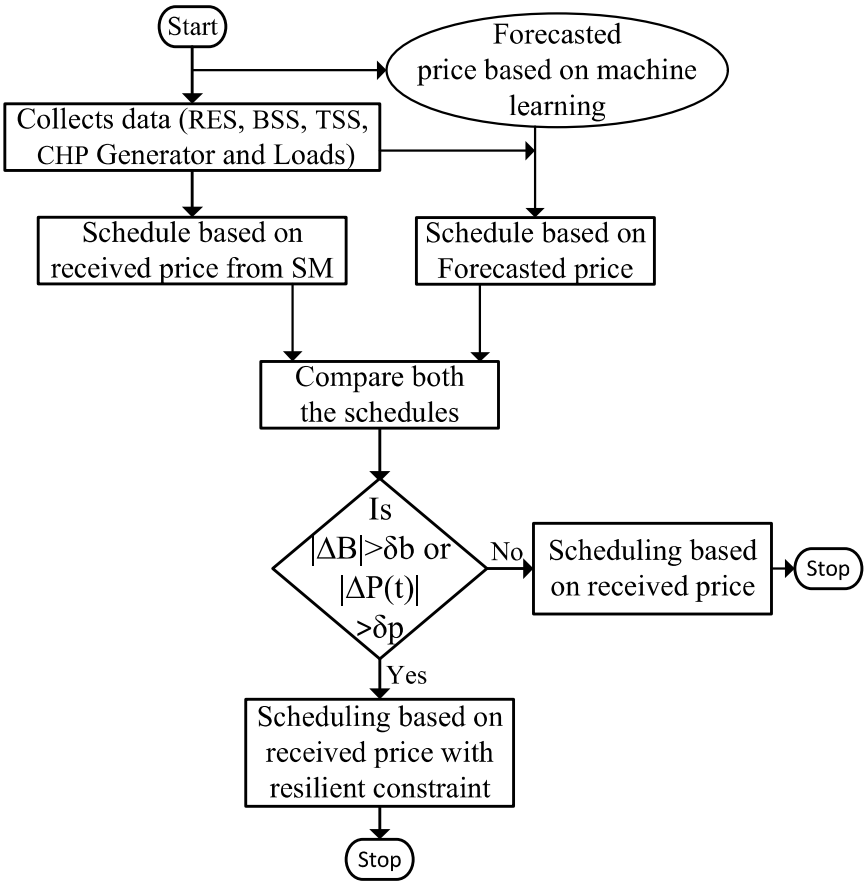

Figure 4.3: Detection Strategy Flowchart

TV, cooker oven, laptop, fluorescent lamp, washing machine, dish washer, tumble dryer, electric vehicle, along with their ratings are given in Table 4.2. 10 kWh battery storage capacity having 10kWh charging/discharging limit and 20 kWh thermal storage capacity having 20kWh charging/discharging limit are installed at each SB. Each smart building is having a CHP generator with specifications as depicted in Table 4.3. The specifications of the renewable energy resources are depicted in Table 4.4. The predicted price which is calculated by using GPR model and price received from the Smart Meter (SM) is shown in Table 4.1. The Figure 4.4 shows the total power generated from renewable energy sources i.e., solar PV and wind turbine of each smart building. The price of natural gas, λ_g, is taken as 2.7 ₹/kWh, where as the maintenance cost of battery, λ_{bmc}, is taken as 0.5 ₹/kWh. Maximum demand limit, P_{mdl}, for each SB is taken as 15kW. GAMS environment is used to implement the proposed Mixed Integer Quadratic Constraint Programming (MIQCP) problem with CPLEX solver to solve the problem.

Table 4.2: Specification of Components in Smart Home

Sl.No	Appliance	Length of Operation (Hour)	$P_{rated}(kW)$
1	Refrigerator	24	0.3
2	Laptop	2	0.1
3	TV	3	0.3
4	Fluorescent Lamp	6	0.84
5	Dish Washer	2	2.1
6	Washing Machine	2	2.1
7	Cooker Hob	1	3
8	Tumble Dryer	2	4
9	Cooker Oven	1	5
10	Microwave	1	1.7
11	Vaccum Cleaner	1	1.2
12	Electric Vehicle	3	3.5

Table 4.3: Name plate of CHP Generator

SB	Capacity (kW)	Power Ratio	efficiency
1	20	1.3	35
2	20	1.2	40
3	40	1.3	35

Table 4.4: Specification.

Sl.No	Components	Rating	Count	Total rating
1	Solar PV	0.1 kw	24	2.4 kW
2	Wind turbine	1 kw	2	2 kW

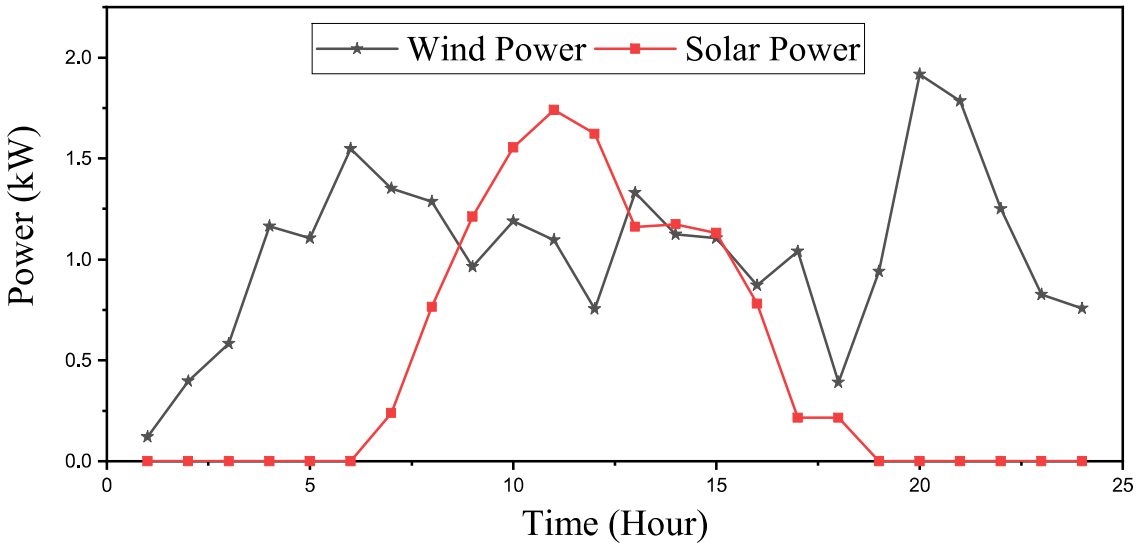

Figure 4.4: RES Generation

4.4.1 Electricity Bill Minimization

Three cases are considered in grid connected smart building energy management system, i.e., scheduling without FDI attack ($CaseI$), scheduling with FDI attack ($CaseII$) and resilient scheduling under FDI attack ($CaseIII$). The scheduled demand of these three cases are shown in the Figure 4.5. It is observed that FDI attack manipulates the demand of each SB such that demand increases during high tariff periods and decreases during low tariff periods. It is observed from Figure 4.5 that due to FDI attack, SB1 demand increases during the high tariff periods i.e., 7:00, 18:00, 19:00 and decrease during the low tariff periods i.e., 5:00, 15:00, 17:00. That is, SB1 demand increases from 0.6 kW to 4.1 kW at 7:00 hours whereas, the demand reduces from 4.1 kW to 0.6 kW at 5:00 hour in $caseII$ as compared to $caseI$. Similarly, due to FDI attack, SB2 demand increases during the high tariff periods i.e, 18:00, 19:00, 20:00 and decreases during the low tariff periods i.e., 5:00, 14:00, 17:00. That is, SB2 demand increases from 5.68 kW to 8.18 kW at 19:00 hour whereas the demand reduces from 4.9 kW to 0.9 kW at 5:00 hour in $caseII$ as compared to $caseI$. Also SB3 demand increases during the high tariff periods i.e., 7:00, 9:00, 12:00, 19:00 hours and decreases during the low tariff periods i.e., 3:00, 5:00, 16:00 hours. That is, SB3 demand increases from 0.9 kW to 4.4 kW at 7:00 hour whereas demand reduces from 12.24 kW to 1.74 kW at 3:00 hour in $caseII$ as compared to $caseI$. Thus, it concluded that consumer pay high electricity bill due to presence of

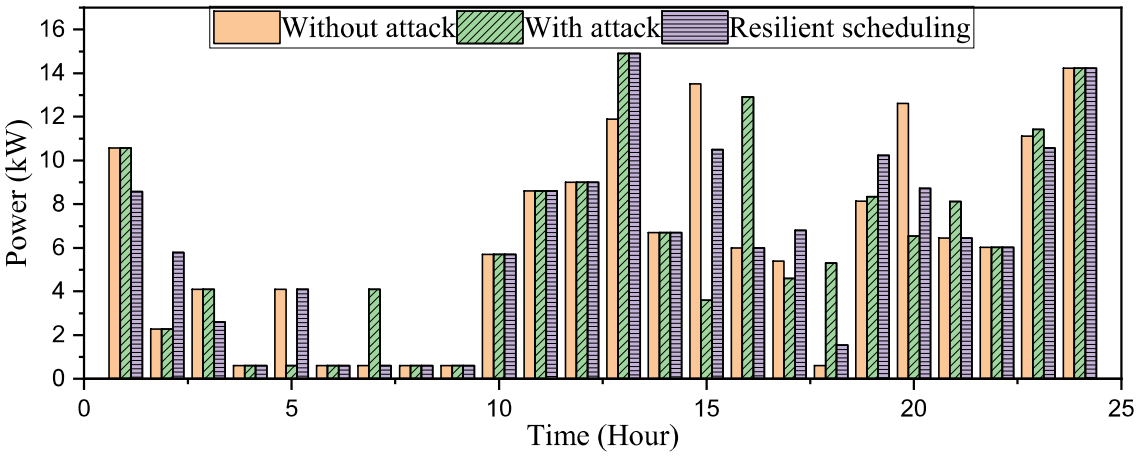

(a) SB1

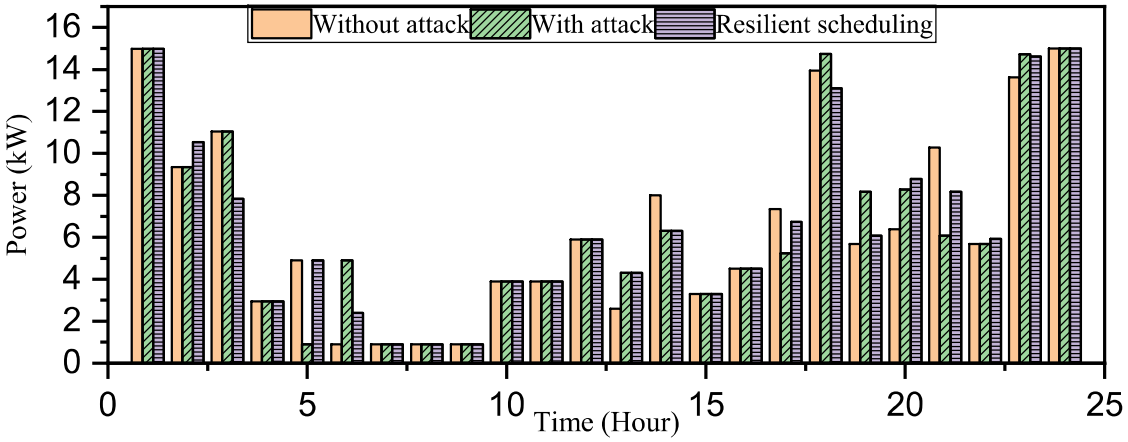

(b) SB2

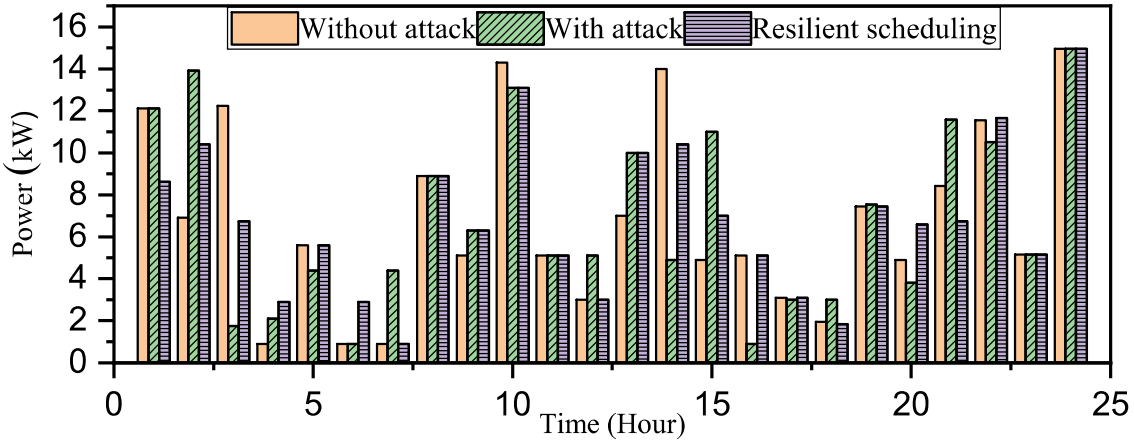

(c) SB3

Figure 4.5: Demand with and without Attack, and Resilient Scheduling

FDI attack in price signal. But in $caseIII$, the consumer does not consume much power because in resilient scheduling the load scheduling of the consumer depends not only on the attacked price but also on the consumer's past consumption pattern. It is also seen from the Figure 4.5 that the demand consumption pattern does not change unexpectedly in $caseI$ and $caseIII$: i.e., for SB1, at 5:00, 7:00, 13:00 and 20:00 hours demand does not change. For example, at 5:00 hour, demand without attack is 4.1 kW and with resilient scheduling is 4.1 kW which shows that in both the cases demand remains same. Where as, at 5:00, 13:00 and 14:00 hours demand in both the cases for SB2 do not change. That is, at 13:00 hour, demand without attack was 2.6 kW and with resilient scheduling, demand is 2.6 kW. For SB3, at 9:00, 10:00, 12:00, and 16:00 hours, demand in both the cases remains unchanged indicating that resilient scheduling is effective under FDI attack.

The import and export power from the grid under these three cases is shown in the Figure 4.6. It is observed from the Figure 4.6 that, SBs import power from the grid for particular interval in $caseI$ while in $caseII$, for same time of interval SBs export power to the grid. For example, at 7:00 hour, SB1 export 3.286 kW to the grid in $caseI$ but in $caseII$, SB1 import 3.041 kW from the grid. Similarly, at 18:00 hour, SB2 export 1.06kW to the grid in $caseI$ but in $caseII$, it imports 4.935 kW from the grid. And also for SB3, at 7:00 hours, smart building exports 3.064 kW to the grid for without attack while it imports 3.674 kW from the grid with attack. Thus, it concluded that the FDI attack affects the grid power exchange. But the import and export power in $caseIII$ almost remains same as in $caseI$ which shows that resilient scheduling is an effective solution against the FDI attack.

4.4.2 FDI Attack analysis

Two cases i.e., $CaseI$ (without FDI attack) and $CaseII$ (with FDI attack) are discussed in this section. Table 4.5 shows the maximum change in demand of each smart building under these two cases. It can be observed that, at the 15^{th} time interval for SB1, demand is 13.5 kW in $CaseI$ where as, it is 3.6 kW in $CaseII$. That is, maximum change (9.9 kW) in demand occurs at the 15^{th} time interval for SB1. Similarly, the maximum change in demand for SB2 and SB3 occurs at the 21st and 3rd intervals, respectively, and maximum change in demand are 4.2 kW and 10.5kW, respectively. Hence it is seen from the Table 4.5 that this huge difference indicates the presence of FDI attack in the system.

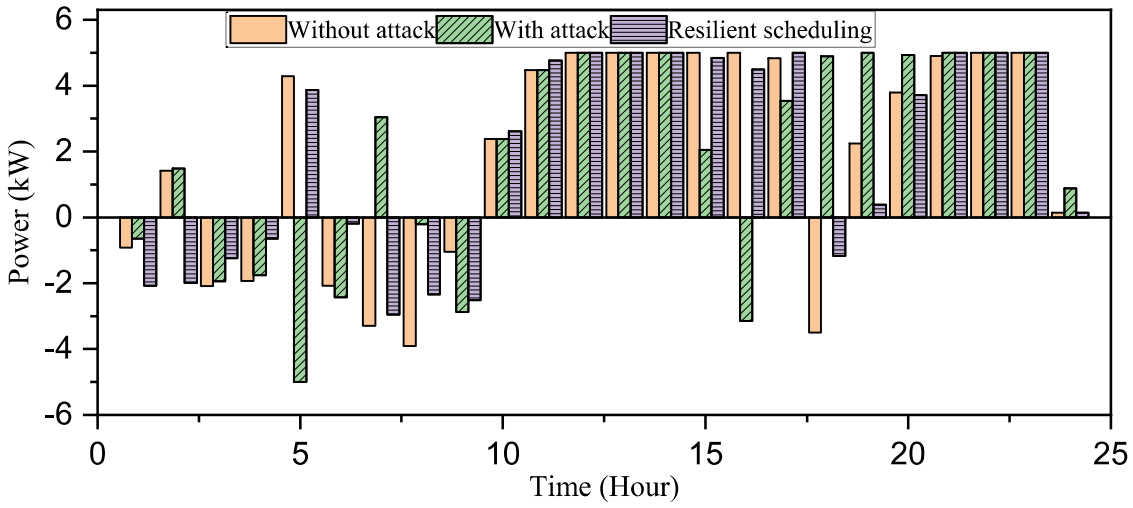

(a) SB1

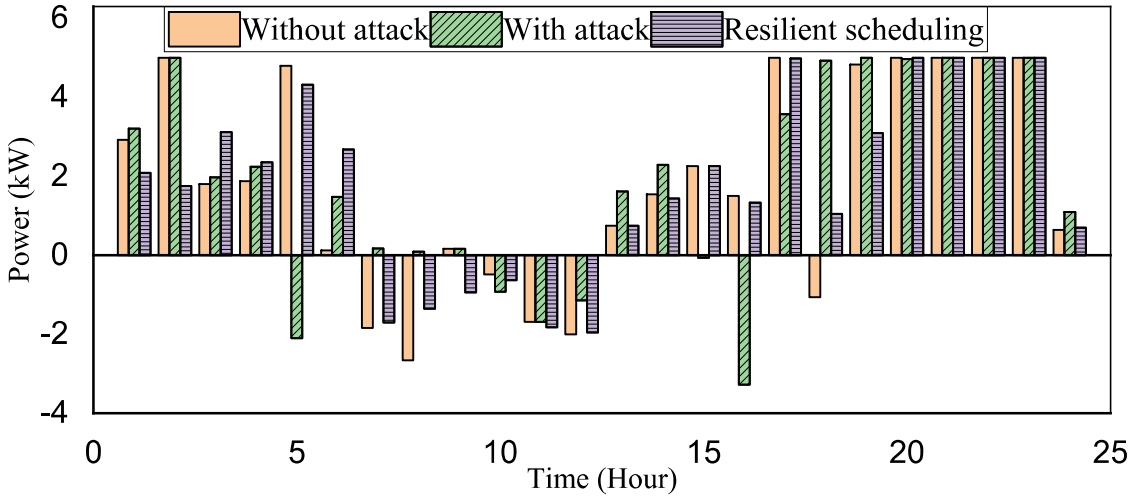

(b) SB2

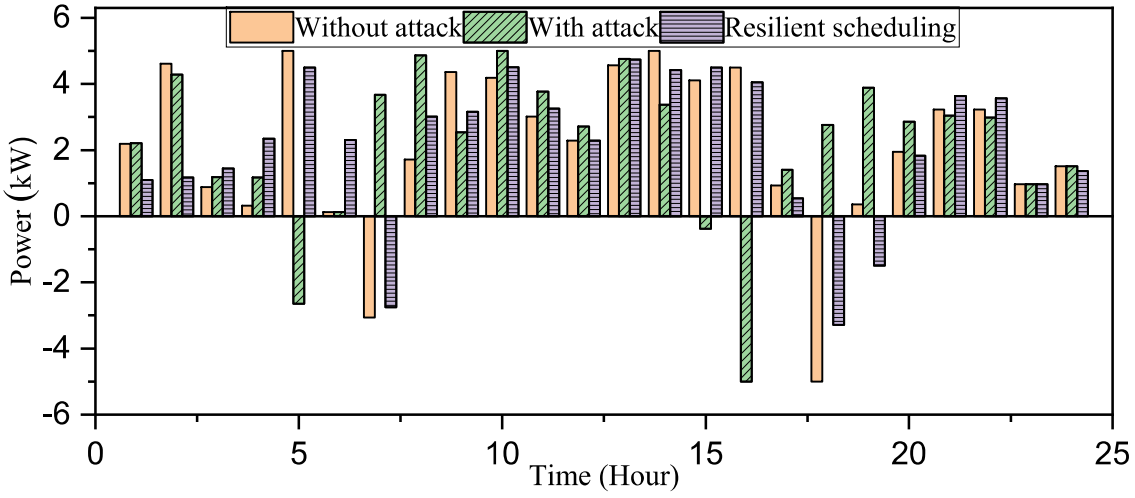

(c) SB3

Figure 4.6: Import and Export Power with, and without Attack, and Resilient Scheduling

Table 4.5: Maximum Change in Demand

SBs	Demand (kW) without attack (interval)	Demand (kW) with attack (interval)	Maximum change in demand (kW)
1	13.5 (15)	3.6 (15)	9.9
2	10.28 (21)	6.08 (21)	4.2
3	12.24 (3)	1.74 (3)	10.5

Electricity bills, B, and rate of change of bills, ΔB, are given in Table 4.6 for $caseI$ and $caseII$ of each SB. It is observed from Table 4.6 that the value of ΔB is greater than the predetermined tolerance value δb. The values of ΔB for SB1, SB2, and SB3 are 7.15%, 4.35%, and 6.54%, respectively. Such sudden changes in bills and consumer behavior is unexpected, which shows that there is some malicious activity in Real Time Price (RTP). From the given Table 4.6, it is observed that electricity bill in $caseIII$ are ₹396.520, ₹411.44, and ₹430.903 for SB1, SB2, and SB3, respectively while in $caseI$ it is ₹395.082, ₹410.006, and ₹429.209 for SB1, SB2, and SB3, respectively. The electricity bill in $caseIII$ is nearly equal to the electricity bill in $caseI$ which shows the effectiveness of the resilient scheduling.

In addition, we have considered the following FDI attacks (i) $caseIV$: scheduling considering FDI attack on demand data, (ii) $caseV$: scheduling considering FDI attack on price and demand (coordinated) data, (iii) $caseVI$: resilient scheduling considering FDI attack on demand data, and (iv) $caseVII$: resilient scheduling considering FDI attack on price and demand (coordinated) data. The electricity bill in, $caseIV$, $caseV$, $caseVI$ and $caseVII$ are given in Table 4.7. From this Table, it is found that electricity

Table 4.6: Electricity Bill Comparison

SBs	Electricity bill (₹) without attack	Electricity bill (₹) with attack	Electricity bill (₹) with resilient scheduling	ΔB in %
1	395.082	423.335	396.52	7.15
2	410.006	427.864	411.44	4.35
3	429.209	457.320	430.903	6.54

Table 4.7: Bill with Attack on Demand data and Attack on Price and Demand data (Coordinated)

SBs	Bill (₹) without attack	Bill (₹) with		Resilient scheduling Bill (₹)	
		Demand attack	Coordinated (price & demand) attack	Demand attack	Coordinated (price & demand) attack
1	395.082	415.52	425.55	398.397	397.571
2	410.006	421.11	426.19	413.192	412.574
3	429.209	448.31	455.21	430.837	430.814

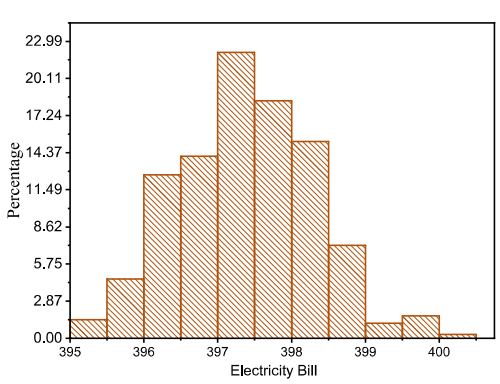

(a) SB1

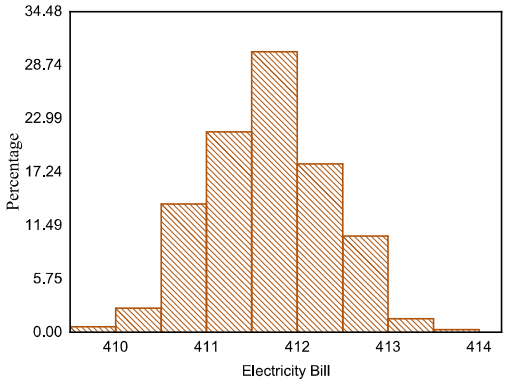

(b) SB2

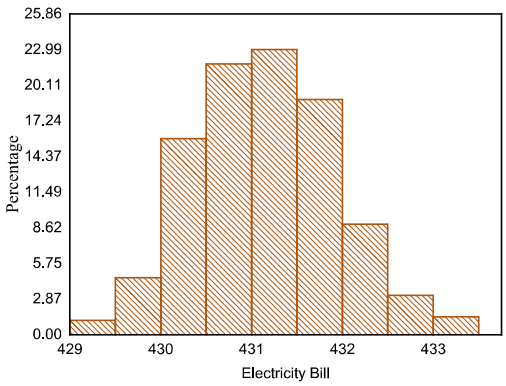

(c) SB3

Figure 4.7: PDF of Electricity bill

bill in $caseI$ is ₹395.082 and in $caseVI$ is ₹398.397 for SB1 which are almost same in both the cases. Similarly, electricity bill in $caseI$ and $caseVII$ are nearly same which shows the efficacy of the proposed resilient scheduling against the FDI attack on demand data as well as coordinated (price and demand data) FDI attack.

To measure the variations in electricity bills, the probability density function (PDF) of the electricity bill is obtained by performing the experiment multiple executions (1000 times) in the case of a coordinated (price and demand data) FDI attack. The PDF of electricity bills of SBs are shown in Figure 4.7. The PDFs of electricity bills can be described using normal distribution $\mathcal{N}(\mu, \sigma)$; where μ and σ are mean and standard deviation. The estimated parameters for PDFs of electricity bill of SB1, SB2, and SB3 are $\mathcal{N}(397.387, 0.922223)$, $\mathcal{N}(411.686, 0.685499)$, and $\mathcal{N}(431.144, 0.770256)$, respectively.

4.5 Summary

A game-theory based multiple smart building energy management system has been formulated with the objective of reducing electricity bill of each smart building. The proposed electricity bill minimization approach is resilient under FDI attack. The results show that detection algorithm based on rate of change in electricity bill and an additional algorithm based on maximum change in demand are sensitive towards FDI attack detection. The resilient scheduling algorithm based on export and import power from the grid and past behaviour of consumer is also an effective solution against FDI attack in the proposed problem formulation. It is observed from the above studies that the electricity bill of the system without resilient scheduling is ₹429.209 whereas the electricity bill in attacked system with resilient scheduling is ₹431.166, which shows the efficacy of the proposed work.